Psychological Medicine

cambridge.org/psm

Cerebral blood flow changes and their genetic mechanisms in major depressive disorder: a combined neuroimaging and transcriptome study

Xuetian Sun[1,2,3,*], Weisheng Huang[1,2,3,*], Jie Wang[1,2,3,*], Ruoxuan Xu[1,2,3], Xiaohan Zhang[1,2,3], Jianhui Zhou[1,2,3], Jiajia Zhu[1,2,3] and Yinfeng Qian[1,2,3]

[1]Department of Radiology, The First Affiliated Hospital of Anhui Medical University, Hefei 230022, China; [2]Research Center of Clinical Medical Imaging, Anhui Province, Hefei 230032, China and [3]Anhui Provincial Institute of Translational Medicine, Hefei 230032, China

Original Article

*These authors contributed equally to this work.

Cite this article: Sun X, Huang W, Wang J, Xu R, Zhang X, Zhou J, Zhu J, Qian Y (2023). Cerebral blood flow changes and their genetic mechanisms in major depressive disorder: a combined neuroimaging and transcriptome study. *Psychological Medicine* **53**, 6468–6480. https://doi.org/10.1017/S0033291722003750

Received: 1 June 2022
Revised: 22 November 2022
Accepted: 28 November 2022
First published online: 5 January 2023

Key words:
Cerebral blood flow; gene expression; major depressive disorder; meta-analysis; neuroimaging

Authors for correspondence:
Yinfeng Qian, E-mail: liangminqyf@sohu.com;
Jiajia Zhu, E-mail: zhujiajiagraduate@163.com

Abstract

Background. Extensive research has shown abnormal cerebral blood flow (CBF) in patients with major depressive disorder (MDD) that is a heritable disease. The objective of this study was to investigate the genetic mechanisms of CBF abnormalities in MDD.

Methods. To achieve a more thorough characterization of CBF changes in MDD, we performed a comprehensive neuroimaging meta-analysis of previous literature as well as examined group CBF differences in an independent sample of 133 MDD patients and 133 controls. In combination with the Allen Human Brain Atlas, transcriptome-neuroimaging spatial association analyses were conducted to identify genes whose expression correlated with CBF changes in MDD, followed by a set of gene functional feature analyses.

Results. We found increased CBF in the reward circuitry and default-mode network and decreased CBF in the visual system in MDD patients. Moreover, these CBF changes were spatially associated with expression of 1532 genes, which were enriched for important molecular functions, biological processes, and cellular components of the cerebral cortex as well as several common mental disorders. Concurrently, these genes were specifically expressed in the brain tissue, in immune cells and neurons, and during nearly all developmental stages. Regarding behavioral relevance, these genes were associated with domains involving emotion and sensation. In addition, these genes could construct a protein-protein interaction network supported by 60 putative hub genes with functional significance.

Conclusions. Our findings suggest a cerebral perfusion redistribution in MDD, which may be a consequence of complex interactions of a wide range of genes with diverse functional features.

Introduction

Major depressive disorder (MDD) is a highly prevalent and disabling mental disorder with significant morbidity, mortality, and cost (Bromet et al., 2011; Greenberg et al., 2021; Kessler & Bromet, 2013; Whiteford et al., 2013). The World Health Organization projected that MDD will be the leading cause of global disease burden by 2030 (World Health Organization, 2008). Although substantial efforts have been made in the past decades, the etiology of MDD remains elusive. Advances in neuroimaging techniques have made it increasingly feasible to investigate the neuropathology of MDD. Benefiting from the ability to precisely map function to underlying neuroanatomy, functional neuroimaging is crucial for studying brain function in health and disease. Cerebral blood flow (CBF), normally coupled to brain metabolism and neuronal activity, is one of the most frequently used and physiologically relevant functional measures (Buxton, 2021; Lecrux, Bourourou, & Hamel, 2019). Positron emission tomography (PET) and single photon emission computed tomography (SPECT) have traditionally been adopted to measure CBF (Wintermark et al., 2005). Arterial spin labeling (ASL), a noninvasive magnetic resonance imaging (MRI) technique, can rapidly quantify CBF using magnetically labeled arterial blood water as an endogenous tracer (Haller et al., 2016; Hernandez-Garcia, Lahiri, & Schollenberger, 2019). With use of these techniques, numerous studies have shown CBF changes in MDD patients (Bench et al., 1992; Cantisani et al., 2016; Chen et al., 2016; Cooper et al., 2020; Duhameau et al., 2010; Ho et al., 2013; Jarnum et al., 2011; Kaichi et al., 2016; Krausz et al., 2007; Li et al., 2018; Lui et al., 2009; Monkul et al., 2012; Ota et al., 2014; Périco et al., 2005; Sahib et al., 2020; Savitz et al., 2012; Vardi et al., 2011; Vasic et al., 2015), establishing CBF as a potential imaging biomarker of this disorder.

© The Author(s), 2023. Published by Cambridge University Press

Despite the extensive research on CBF alterations in MDD, the results of those investigations vary considerably, with inconsistency in both location and direction of effects. These heterogeneous results may be partially due to limited statistical power from relatively small samples, clinical heterogeneity related to illness profile variation, and methodological differences. In this framework, neuroimaging meta-analysis emerges as a potent approach to synthesizing the multitude of results from published imaging literature in an unbiased manner, with the advantages of enlarging sample size, increasing power, and separating the consistent findings from those occurring by chance (Muller et al., 2018). Although there have been prior neuroimaging meta-analyses examining CBF abnormalities in MDD (Chen et al., 2015; Chithiramohan et al., 2022; Hamilton et al., 2012; Li et al., 2017; Wang & Yang, 2022), a rapidly increasing number of recent publications in the field along with continuing improvements in meta-analytic methods (Albajes-Eizagirre, Solanes, Vieta, & Radua, 2019b) have allowed us to attempt a more thorough characterization of CBF changes in MDD.

MDD is a moderately heritable disease with an estimated genetic heritability of ~40% (Corfield, Yang, Martin, & Nyholt, 2017; Sullivan, Neale, & Kendler, 2000). Identifying genetic risk factors for MDD may not only improve our understanding of its pathogenesis, but also inform earlier and more reliable disease detection. Large-scale human genome-wide association studies have identified multiple risk variants, genes, and gene-sets in association with MDD (Consortium, 2015; Howard et al., 2018, 2019; Hyde et al., 2016; Ripke et al., 2013; Wray et al., 2018). Furthermore, a recent transcriptome study found brain gene expression alterations in MDD (Gandal et al., 2018), offering integrated insight into how genetic variants interact with environmental and epigenetic risk factors in the brain to confer risk for MDD. Despite these promising findings, relatively little is known about the exact genetic mechanisms of certain disease phenotypes in MDD, such as CBF changes.

A combined analysis of brain imaging data and brain-wide gene expression atlases such as the Allen Human Brain Atlas (AHBA) (Hawrylycz et al., 2012) has given rise to the emergent domain of neuroimaging transcriptomics, which provides a workable route towards the identification of genes with spatial profiles of regional expression that track anatomical variations in a certain neuroimaging phenotype (Chen et al., 2022; Fornito, Arnatkeviciute, & Fulcher, 2019; Liu et al., 2022; Zhang et al., 2021), laying the foundation for bridging the gap between microscale molecular function and macroscale brain organization. In this domain, there has been growing interest in examining the spatial associations between disease neuroimaging phenotypes and brain gene expression, which may help shed light on the genetic mechanisms underlying imaging biomarkers of mental disorders (Ji et al., 2021; Liu, Tian, Li, Li, & Zhuo, 2019; Romero-Garcia, Warrier, Bullmore, Baron-Cohen, & Bethlehem, 2019; Xie et al., 2020). By means of this powerful approach, researchers have discovered several sets of genes whose expression levels are linked to brain structural and functional abnormalities in MDD (Althubaity et al., 2022; Anderson et al., 2020; Li et al., 2021; Xue et al., 2020). Nonetheless, there is still a paucity of transcription-neuroimaging association studies into the genetic mechanisms of CBF changes in MDD.

To elucidate such mechanisms, we initially determined CBF changes in MDD by performing a comprehensive neuroimaging meta-analysis as well as examining group CBF differences in an independent large sample of 133 MDD patients and 133 healthy controls (HC). Notably, compared with the Wang et al., meta-analysis including only ASL studies (Wang & Yang, 2022), our meta-analysis included studies from both ASL and PET/SPECT. In combination with the AHBA, transcriptome-neuroimaging spatial correlation analyses were then conducted to identify genes whose expression patterns were associated with CBF changes in MDD. Finally, a set of post hoc analyses [i.e. functional enrichment, specific expression, behavioral relevance, and protein-protein interaction (PPI) analyses] were carried out for the identified genes to describe their functional features. A schematic overview of the study design and analysis pipeline is shown in Fig. 1.

Materials and methods

Literature search and selection

Our meta-analysis was conducted according to the Preferred Reporting Items for Systematic Reviews and Meta-Analyses (PRISMA) guidelines (Moher, Liberati, Tetzlaff, Altman, & Group, 2009). A systematic search was performed independently by two investigators (X.S. and W.H.) to determine relevant studies published in PubMed and Web of Science before 19 February 2021. This meta-analysis protocol was pre-registered in PROSPERO (https://www.crd.york.ac.uk/PROSPERO/, registration number: CRD42021250728). The search terms along with the inclusion and exclusion criteria can be found in the Supplementary materials. The detailed study selection process is shown in online Supplementary Fig. S1. For each included study, we recorded the following information: scanner, sample size, sex, age, symptom severity, diagnostic criteria, and illness duration.

Neuroimaging meta-analysis of group CBF differences

Voxel-wise meta-analysis of CBF differences between MDD patients and HC was conducted using Seed-based *d* Mapping with Permutation of Subject Images (SDM-PSI, version 6.21) (https://www.sdmproject.com). In contrast to the traditional activation likelihood estimation (ALE) method, SDM-PSI enables investigators to combine both peak coordinates and statistical parametric maps and uses standard effect size and variance-based meta-analytic calculations. The SDM method has been described in detail elsewhere (Albajes-Eizagirre et al., 2019a). First, we extracted peak coordinates and corresponding effect sizes (e.g. *t* values) of clusters with significant CBF differences between MDD patients and HC from each study. Coordinates reported in the Talairach space were converted to the Montreal Neurological Institute (MNI) space using the matrix transformations proposed by Lancaster (Lancaster et al., 2007); *z* or *p* values were converted to *t* values using SDM online conversion utilities (https://www.sdmproject.com/utilities/?show=Statistics). Then, a standard MNI map of CBF differences between MDD patients and HC was separately created for each study using a Gaussian kernel of 20 mm full width at half maximum (Radua et al., 2012). Next, these maps were combined using a standard random-effects model accounting for sample size, intra-study variability and between-study heterogeneity, resulting in a final map of group CBF differences (*z* map) for all included studies. Considering the relatively small number of included studies, we reported results using a voxel-wise threshold of $p < 0.005$ combined with a cluster size threshold of 10 voxels to optimally balance Types I and II error rates (Lieberman & Cunningham, 2009;

https://doi.org/10.1017/S0033291722003750 Published online by Cambridge University Press

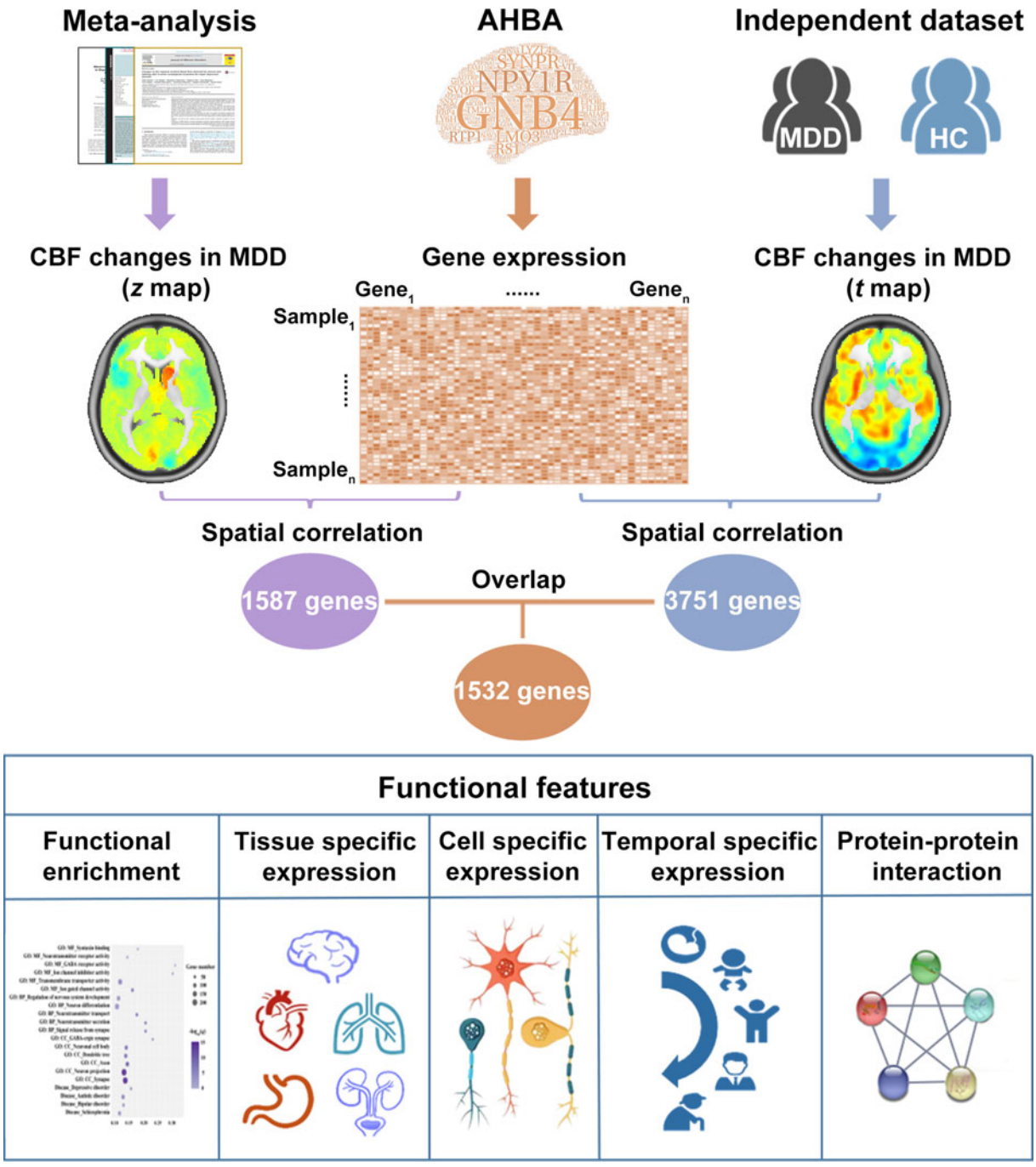

Fig. 1. A schematic overview of the study design and analysis pipeline. AHBA, Allen Human Brain Atlas; CBF, cerebral blood flow; HC, healthy controls; MDD, major depressive disorder.

Radua et al., 2012). Several supplementary analyses were pursued to test the robustness and reliability of our meta-analysis results. Detailed steps are described in the Supplementary materials.

Participants in the independent dataset

Group CBF differences were also tested in an independent sample of 133 MDD patients and 133 well-matched HC. MDD patients were enrolled consecutively from the inpatient and outpatient departments of Hefei Fourth People's Hospital. HC were recruited from the local community via poster advertisements. This study was conducted in accordance with the Declaration of Helsinki and was approved by the ethics committee of The First Affiliated Hospital of Anhui Medical University (5101152). Written informed consent was obtained from all participants after they had been given a complete description of the study. Inclusion and exclusion criteria for all participants are described in the Supplementary materials.

MRI data acquisition and CBF analysis

MRI data were acquired on a 3.0-Tesla MR system (Discovery MR750w, General Electric, Milwaukee, WI, USA). The resting-state perfusion imaging was performed using a pseudo-

https://doi.org/10.1017/S0033291722003750 Published online by Cambridge University Press

continuous ASL sequence with a 3D fast spin-echo acquisition and background suppression. Detailed scan sequences and parameters can be found in the Supplementary materials. Three ASL difference images were calculated by subtracting the label images from the control images and then averaged. Next, CBF was quantified by applying a single-compartment model (Buxton et al., 1998) to the mean ASL difference and proton-density-weighted reference images (Xu et al., 2010; Zhu et al., 2015, 2017; Zhuo et al., 2017). The Statistical Parametric Mapping software (SPM12, http://www.fil.ion.ucl.ac.uk/spm) was used to normalize the CBF images into the MNI space. The detailed steps are described in the Supplementary materials. For the independent dataset, CBF differences between MDD patients and HC were examined using a two-sample t test in a voxel-wise manner, resulting in a statistical t map. Multiple comparisons were corrected using the cluster-level family-wise error (FWE) method, resulting in a cluster defining threshold of $p < 0.001$ and a corrected cluster significance of $p < 0.05$.

Brain gene expression data processing

Brain gene expression data were obtained from the downloadable AHBA dataset (http://www.brain-map.org) (Hawrylycz et al., 2012, 2015). The dataset was derived from six human postmortem donors (online Supplementary Table S1). The original expression data of more than 20 000 genes at 3702 spatially distinct brain tissue samples were processed using a newly proposed pipeline (Arnatkeviciute, Fulcher, & Fornito, 2019). The detailed steps can be found in the Supplementary materials. After these processing procedures, we obtained normalized expression data of 5013 genes for 1280 tissue samples. Because our neuroimaging meta-analysis was performed within a gray matter mask provided by the SDM-PSI, we further restricted our analyses to the samples within this mask, resulting in a final sample × gene matrix of 894×5013.

Transcription-neuroimaging association analysis

To derive the group CBF difference in a given brain tissue sample, we drew a spherical region (radius = 3 mm) centered at the MNI coordinate of this sample and extracted the average z value of voxels within the sphere from the meta-analysis z map. Then, cross-sample (894 samples) Pearson's correlations between gene expression and z values were performed in a gene-wise manner (5013 genes), yielding 5013 correlation coefficients. Multiple comparisons were corrected using the Bonferroni method ($p < 0.05/5013 = 9.974 \times 10^{-6}$). Likewise, the above-described analysis procedure was conducted for the t map in the independent dataset. Then, only genes with significant spatial correlations with both the meta-analysis z map and the independent dataset t map were considered as the genes whose expression levels were associated with CBF changes in MDD patients. To further test whether the number of the identified genes was significantly greater than the random level, a spatially-constrained permutation test was conducted to establish the significance of our results. The detailed steps are described in the Supplementary materials.

Gene enrichment analysis

A series of enrichment analyses were conducted for the identified genes associated with CBF changes in MDD patients. First, functional annotation was carried out with use of the ToppGene portal (https://toppgene.cchmc.org/) (Chen, Bardes, Aronow, & Jegga, 2009). Gene ontology (GO) was used to determine the biological functions including molecular functions (MFs), biological processes (BPs), and cellular components (CCs). The disease database was adopted to determine the related diseases. Second, we used online tissue-specific expression analysis (http://genetics.wustl.edu/jdlab/tsea/) and cell type-specific expression analysis (http://genetics.wustl.edu/jdlab/csea-tool-2/) (Dougherty, Schmidt, Nakajima, & Heintz, 2010) tools to conduct tissue, cell type, and temporal specific expression analyses, with the aim of determining the specific tissues, cortical cell types, and developmental stages in which these genes were overrepresented. A specificity index probability (pSI) was used to determine how likely a gene was to be specifically expressed (Xu, Wells, O'Brien, Nehorai, & Dougherty, 2014) and four pSI thresholds (0.05, 0.01, 0.001, and 0.0001) were employed in this analysis. Finally, we examined the overlap between the genes associated with CBF changes in MDD patients found in the current study and MDD-associated genes in the MalaCards database (https://www.malacards.org/) (Rappaport et al., 2017), using 20 737 genes with unique Entrez IDs in the AHBA as the background list. For the aforementioned enrichment analyses, Fisher's exact tests were used to test their significance. Multiple testing was corrected using the Benjamini and Hochberg method for false discovery rate (FDR-BH correction) with a corrected p value (q) of 0.05.

Behavioral relevance analysis

To capture the behavioral relevance of the genes related to CBF changes in MDD patients, we tested their associations with behavioral domains from the Neurosynth (https://neurosynth.org/), a well-validated and publicly available platform for meta-analysis of neuroimaging literature (Yarkoni, Poldrack, Nichols, Van Essen, & Wager, 2011). Detailed steps are provided in the Supplementary materials.

Protein-protein interaction analysis

PPI analysis was performed with STRING v11.0 (https://string-db.org/) to determine whether the genes associated with CBF changes in MDD patients could construct a PPI network with a highest confidence interaction score of 0.9. Genes with the top 10% highest degree values (i.e. the number of edges connected to a gene) were defined as hub genes. In addition, the Human Brain Transcriptome database (http://hbatlas.org/) was employed to delineate the spatial-temporal expression trajectory of hub genes with the highest degree values.

Results

Meta-analysis of CBF changes in MDD patients

After a comprehensive literature search and selection, our neuroimaging meta-analysis included 600 MDD patients and 448 HC from 17 studies. The demographic and clinical characteristics of these participants are shown in Table 1. Compared with HC, MDD patients exhibited increased CBF in the right caudate and decreased CBF in the left insula and right calcarine sulcus (Fig. 2*a* and online Supplementary Table S2). Moreover, jackknife sensitivity analysis (82–88% consistency) (online Supplementary Table S3), publication bias analysis including small-study effect and excess significance tests ($p > 0.05$) (online Supplementary

https://doi.org/10.1017/S0033291722003750 Published online by Cambridge University Press

https://doi.org/10.1017/S0033291722003750 Published online by Cambridge University Press

Table 1. Demographic and clinical characteristics of the 17 studies in the meta-analysis

Study	Type	Subjects (males)		Mean age (years)		Symbol severity (scale type)	Diagnostic criteria-MDD	Scanner	Illness duration (years)
		MDD	HC	MDD	HC				
Ho et al. (2013)	ASL	25 (7)	26 (7)	15.98	16.42	73.3 (Children's Depression Rating Scale)	DSM-IV	3T GE	1.9
Lui et al. (2009)	ASL	37 (26)	42 (27)	33	37	23 (HRSD)	DSM-IV	3T GE	2
Duhameau et al. (2010)	ASL	6 (4)	6 (3)	52.5	47.17	22.5 (HRSD)	DSM-IV	3T Philips	NA
Monkul et al. (2012)	PET	20 (5)	21 (7)	37.2	34.8	22 (HAMD)	DSM-IV	GE	NA
Bench et al. (1992)	PET	33 (21)	23 (10)	56.8	63.4	25 (HAMD)	NA	NA	NA
Vasic et al. (2015)	CASL	43 (17)	29 (11)	37.1	34.5	20.9 (HAMD)	DSM-IV	3T Siemens	7.2
Krausz et al. (2007)	SPECT	10 (1)	10 (1)	49.1	49.7	NA	DSM-IV	NA	NA
Kaichi et al. (2016)	pCASL	53 (27)	36 (17)	42.27	39.87	20.4 (HRSD)	DSM-IV	3T GE	NA
Cooper et al. (2020)	ASL	106 (39)	36 (12)	37.65	37.49	18.92 (HAMD)	DSM-IV	3T (Siemens GE Philips)	NA
Cantisani et al. (2016)	ASL	20 (10)	19 (8)	43.3	41.05	25.45 (HAMD) 26.65 (MADRS)	DSM-IV	3T Siemens	10.7
Savitz et al. (2012)	PET	66 (25)	79 (34)	36.3	34.2	24.2 (MADRS)	DSM-IV	NA	16.9
Vardi et al. (2011)	SPECT	37 (16)	27 (13)	49.81	55.04	31.53 (HAMD)	DSM-IV	Elscint	1.8
Jarnum et al. (2011)	pCASL	23 (7)	26 (13)	43.2	42	23.3 (HRSD)	DSM-IV	3T GE	NA
Chen et al. (2016)	pCASL	10 (7)	15 (6)	38.7	38.42	35.3 (HAMD)	DSM-IV	3T Philips	NA
Périco et al. (2005)	SPECT	15 (3)	15 (6)	34.5	33.27	26.9 (HRSD)	DSM-IV	Elscint	2.3
Sahib et al. (2020)	pCASL	22 (16)	18 (8)	36.11	35.27	NA	DSM-V	3T Siemens	18.91
Li et al. (2018)	SPECT	74 (21)	20 (8)	41.9	38	25.49 (HAMD)	DSM-IV	GE	NA

ASL, arterial spin labeling; CASL, continuous arterial spin labeling; DSM, diagnostic statistical manual of mental disorders; GE, General Electric Company; HAMD, Hamilton Rating Scale for Depression; HC, healthy controls; HRSD, Hamilton Rating Scale for Depression; MADRS, Montgomery-Asberg Depression Rating Scale; MDD, major depressive disorder; NA, not available; pCASL, pseudo-continuous arterial spin labeling; PET, positron emission tomography; SPECT, single photon emission computed tomography

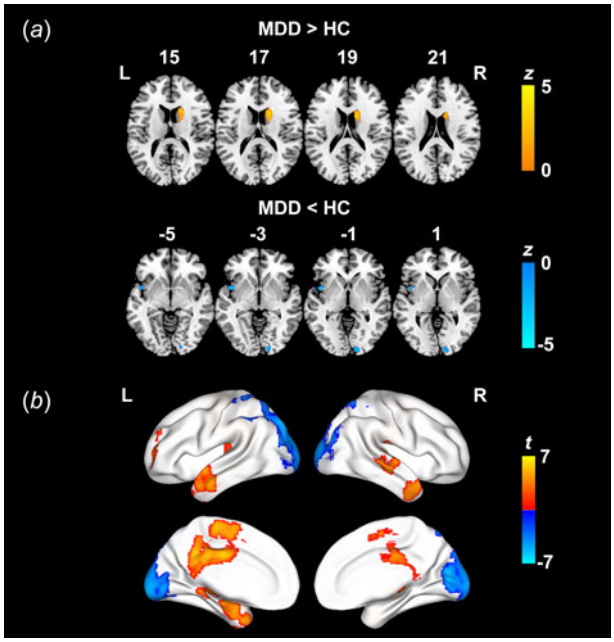

Fig. 2. (*a*) Brain regions with CBF differences between MDD patients and HC identified by the neuroimaging meta-analysis. (*b*) Brain regions with CBF differences between MDD patients and HC in the independent dataset. Warm and cold colors denote increased and decreased CBF in MDD patients, respectively. CBF changes in the subcortical regions are not shown. CBF, cerebral blood flow; HC, healthy controls; MDD, major depressive disorder; L, left; R, right.

Table S4), and heterogeneity analysis ($I^2 < 50\%$) (online Supplementary Table S5) demonstrated the robustness and reliability of our meta-analysis results.

CBF changes in MDD patients in the independent dataset

The demographic and clinical characteristics of the independent sample are presented in Table 2. There were no significant differences in age, gender, and education between MDD patients and HC. The voxel-wise two-sample *t* test revealed a mix of increased and decreased CBF in MDD patients (Fig. 2*b* and online Supplementary Table S6). Specifically, MDD patients showed increased CBF in the bilateral middle cingulate gyrus/bilateral supplementary motor area/left posterior cingulate gyrus/left precuneus, left putamen, right temporal pole, left middle temporal gyrus, right superior temporal gyrus, bilateral thalamus, and left middle frontal gyrus relative to HC ($p < 0.05$, cluster-level FWE corrected). In addition, MDD patients showed decreased CBF in the bilateral occipital cortex extending to bilateral parietal cortex in comparison with HC ($p < 0.05$, cluster-level FWE corrected).

Genes associated with CBF changes in MDD patients

Leveraging transcriptome-neuroimaging spatial correlation analyses, we found that the meta-analysis *z* map and the independent dataset *t* map were respectively associated with expression measures of 1587 and 3751 genes ($p < 0.05$, Bonferroni corrected), with 1532 overlap genes (Supplementary file 1). These overlap genes, whose expression levels were considered to associate with CBF changes in MDD patients, were used for further analyses. The spatially-constrained permutation test showed that none out of 5000 permutations resulted in more genes than those identified using the real data ($P_{perm} < 0.0002$), indicating that our results were different from random. Moreover, we observed significant overlaps between the genes in the main analysis and those identified using two other differential stability (DS) thresholds of 40% (overlap ratio: 97.80%) and 60% (overlap ratio: 96.42%) (online Supplementary Table S7 and file 2).

Gene functional enrichment

To characterize the biological functions and diseases of the genes associated with CBF changes in MDD patients, we performed functional enrichment analyses using the ToppGene portal. The results of functional enrichment are listed in Supplementary file 3 and are depicted in Fig. 3. With regard to GO, these genes were enriched for MFs including syntaxin binding, neurotransmitter receptor activity, GABA receptor activity, ion channel inhibitor activity, transmembrane transporter activity, and ion gated channel activity; for BPs including regulation of nervous system development, neuron differentiation, neurotransmitter transport, neurotransmitter secretion, and signal release from synapse; and for CCs including neuron projection, neuronal cell body, axon, dendritic tree, synapse, and GABA-ergic synapse. As to diseases, these genes were found to be enriched for several common mental disorders including depressive disorder, autistic disorder, bipolar disorder, and schizophrenia.

Tissue, cell type, and temporal specific expression

The specific expression results of the 1532 genes related to CBF changes in MDD patients are listed in Supplementary file 4 and are illustrated in Fig. 4. Tissue specific expression analysis

Table 2. Demographic and clinical characteristics of the independent sample

Characteristics	MDD	HC	Statistics	*p* value
Number of subjects	133	133	–	–
Age (years)	43.5 ± 11.3	45.6 ± 11.2	$t = -1.57$	0.12
Gender (female/male)	87/46	95/38	$\chi^2 = 1.11$	0.29
Education (years)	9.0 ± 3.6	9.6 ± 3.6	$t = -1.49$	0.14
Illness duration (years)	5.4	NA	–	–
HAMD	28.6 ± 12.0	2.0 ± 3.3	$t = 24.78$	<0.001
HAMA	19.7 ± 8.0	2.1 ± 3.5	$t = 23.40$	<0.001

HAMA, Hamilton Rating Scale for Anxiety; HAMD, Hamilton Rating Scale for Depression; HC, healthy controls; MDD, major depressive disorder; NA, not available

https://doi.org/10.1017/S0033291722003750 Published online by Cambridge University Press

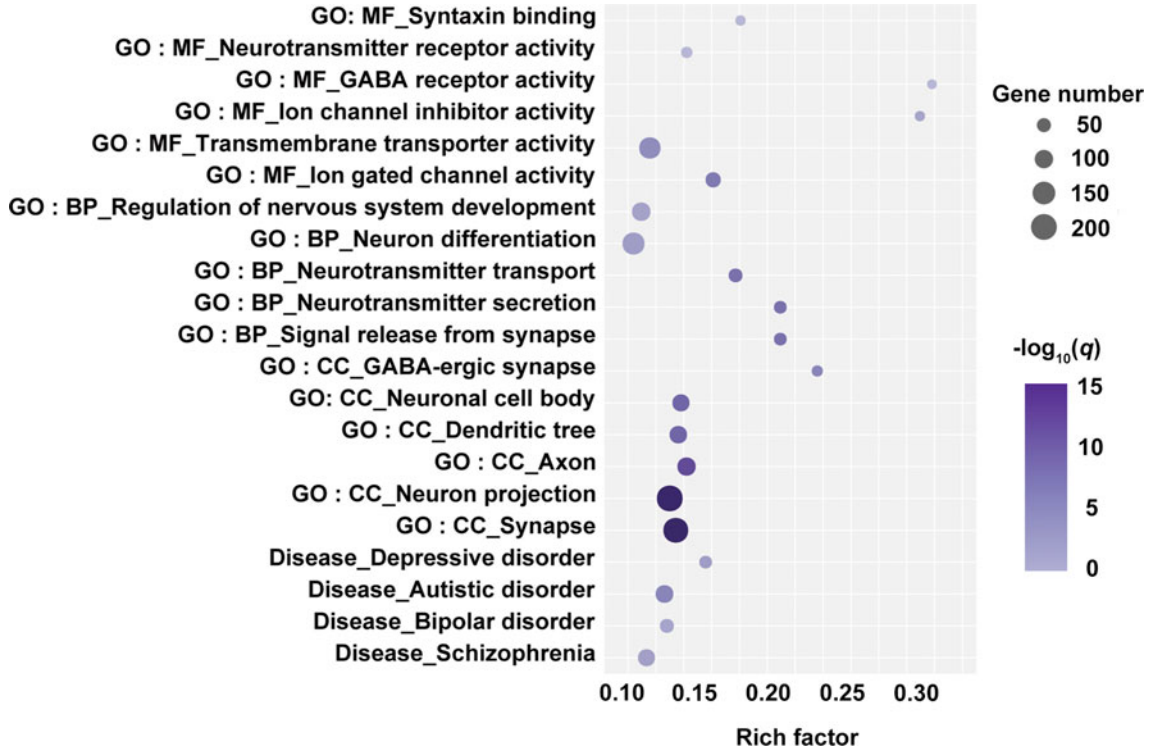

Fig. 3. Functional enrichment of the genes associated with CBF changes in MDD patients. For the bubble chart, the *x*-axis represents the rich factor and the *y*-axis represents items from the GO and disease databases. The rich factor refers to the ratio of the number of the significant genes annotated to the item to the number of all genes annotated to the item. The bubble size denotes the number of genes overlapping with those belonging to each item, and the bubble color represents the $-\log_{10}(q)$. BP, biological process; CBF, cerebral blood flow; CC, cellular component; GO, gene ontology; MDD, major depressive disorder; MF, molecular function.

demonstrated that these genes were specifically expressed in the brain tissue (Fig. 4*a*). Cell type specific expression analysis revealed that these genes were specifically expressed in immune cells and multiple types of neurons including Pnoc+, Ntsr+, Glt25d2, and Cort+ (Fig. 4*b*). Temporal specific expression analysis showed that these genes were preferentially expressed during early mid-fetal, late mid-fetal, late fetal, neonatal and early infancy, early childhood, middle and late childhood, adolescence, and young adulthood (Fig. 4*c*).

Overlap with MDD-associated genes

Fisher's exact test revealed that the 1532 genes associated with CBF changes in MDD patients found in the current study significantly overlapped with the 110 MDD-associated genes in the Malacards database (17 overlap genes, odds ratio = 2.10, $p = 6.26 \times 10^{-3}$).

Behavioral relevance

By linking gene expression with behavioral domains via the Neurosynth, we found that the genes associated with CBF changes in MDD patients were correlated with multiple behavioral terms including visual, emotion, affective, fear, stress, sensory, depression, and anxiety (Fig. 5).

PPI network and hub genes

PPI analysis revealed that 604 genes from the 1532 genes could construct an interconnected PPI network (online Supplementary Fig. S3A). This network consisted of 3582 edges, which was significantly higher than expected ($p = 9.6 \times 10^{-12}$). 60 genes with the top 10% highest degree values were defined as hub genes (Supplementary file 5). In addition, we delineated the spatial-temporal expression trajectory of three hub genes with the highest degree values (i.e. GNG2, GNB4, and GNG4) (online Supplementary Fig. S3B).

Discussion

To our knowledge, this is the first study to investigate the genetic mechanisms of CBF changes in MDD using a combined analysis of brain imaging and gene expression data. Neuroimaging meta-analysis of previous literature and group comparison analysis in an independent dataset consistently demonstrated that MDD patients had increased CBF in the reward circuitry and default-mode network and decreased CBF in the visual system. Moreover, transcriptome-neuroimaging correlation analysis revealed that these CBF changes were spatially associated with expression of 1532 genes, which were enriched for important MFs, BPs, and CCs of the cerebral cortex as well as several common mental disorders. Concurrently, these genes were specifically expressed in the brain tissue, in immune cells and neurons, and during nearly all developmental stages. Regarding behavioral relevance, these genes were associated with domains involving emotion and sensation. In addition, these genes could construct a PPI network supported by 60 putative hub genes with functional significance. Altogether, our findings suggest that CBF changes in MDD may be a consequence of complex interactions of a wide range of genes with diverse functional features, confirming the polygenic nature of this illness.

https://doi.org/10.1017/S0033291722003750 Published online by Cambridge University Press

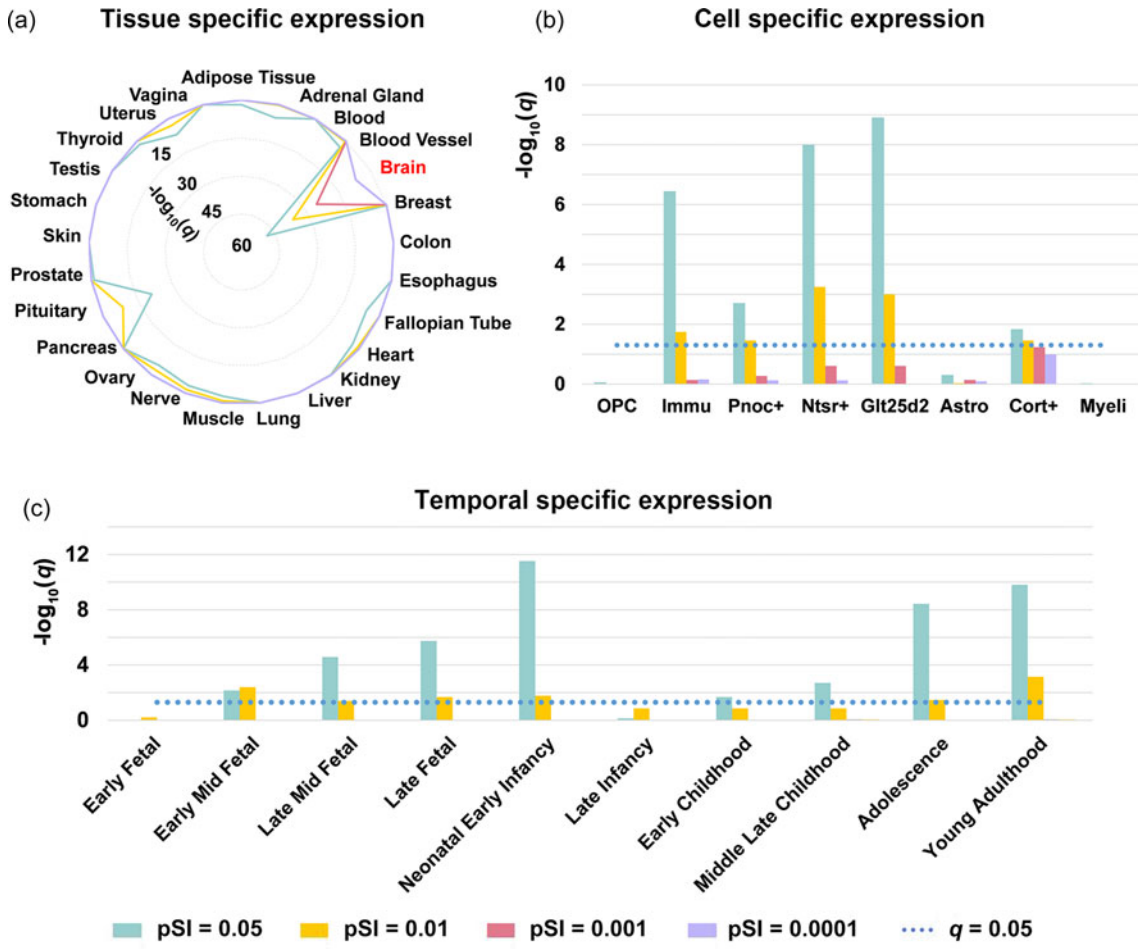

Fig. 4. Specific expression of the genes associated with CBF changes in MDD patients. (*a*) Tissue specific expression. (*b*) Cell specific expression. (*c*) Temporal specific expression. Astro, astrocytes; CBF, cerebral blood flow; Cort+, corticosterone-expressing neurons; Glt25d2, corticopontine neurons; Immu, immune cells; MDD, major depressive disorder; Myeli, myelinating oligodendrocytes; Ntsr+, corticothalamic neurons; OPC, oligodendrocyte progenitor cells; Pnoc+, prepronociceptin-expressing neurons.

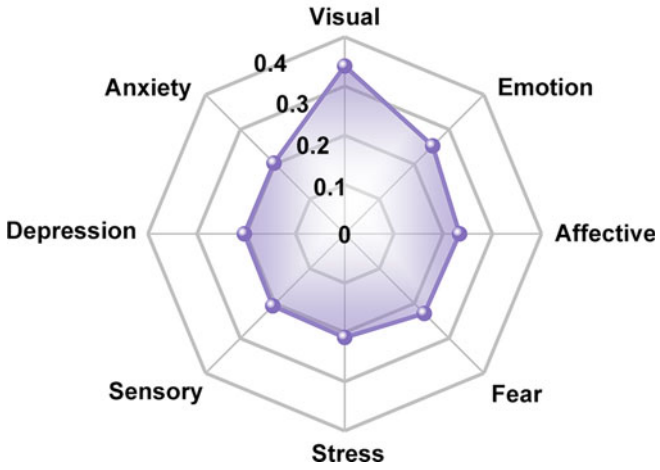

Fig. 5. Behavioral relevance of the genes associated with CBF changes in MDD patients. The radial array numbers represent average absolute correlation coefficients between expression measures of the identified genes and activation values of behavioral terms from the Neurosynth. CBF, cerebral blood flow; MDD, major depressive disorder.

The neuroimaging meta-analysis revealed that MDD patients presented with increased CBF in the caudate and decreased CBF in the insula and calcarine sulcus relative to HC. In the independent dataset, MDD patients showed increased CBF in the middle cingulate gyrus, supplementary motor area, posterior cingulate gyrus/precuneus, putamen, temporal cortex, thalamus and middle frontal gyrus, as well as decreased CBF predominantly in the occipital cortex. These results can be summarized as hyperperfusion in the reward circuitry [the caudate, putamen, and middle frontal gyrus (Clery-Melin, Jollant, & Gorwood, 2019)] and default-mode network (the posterior cingulate gyrus/precuneus, lateral temporal cortex, and thalamus [Buckner & DiNicola, 2019; Raichle, 2015)] and hypo-perfusion in the visual system (the occipital cortex), indicating a perfusion redistribution in the brain of MDD patients. It is well established that MDD is a clinically heterogeneous disorder characterized by a mixture of emotional, cognitive, and neurovegetative symptoms (Malhi & Mann, 2018). Anhedonia represents one of the fundamental emotional symptoms in patients suffering from MDD, which is thought to associate with impaired reward processing possibly arising from dysfunction in the reward circuitry (Hoflich, Michenthaler, Kasper, & Lanzenberger, 2019; Li et al., 2018; Nestler & Carlezon, 2006; Pizzagalli et al., 2009; Russo &

https://doi.org/10.1017/S0033291722003750 Published online by Cambridge University Press

Nestler, 2013). For example, Pizzagalli et al., found caudate dysfunction during reward processing as well as a link between caudate volume and anhedonia in MDD patients (Pizzagalli et al., 2009). Tao and colleagues reported that MDD patients exhibited abnormal function in the 'hate circuit' involving the putamen and prefrontal cortex, which may reflect reduced cognitive control over negative feelings toward both self and others (Tao et al., 2013). Rumination, defined as repetitive thinking about negative information, is a characteristic of MDD (Whitmer & Gotlib, 2013). The default-mode network is classically considered an 'intrinsic' system, specializing in internally oriented cognitive processes such as daydreaming, reminiscing and future planning (Yeshurun, Nguyen, & Hasson, 2021). There is empirical evidence from functional neuroimaging pointing to an intimate link between rumination and activations of the default-mode network (Zhou et al., 2020). Our observation of decreased CBF in the visual system is coherent with previous reports (Bonte et al., 2001; Nagafusa et al., 2012). It is largely known that the visual system is not only implicated in visual processing (Prasad & Galetta, 2011), but also engaged by higher level cognitive processes (Roelfsema & de Lange, 2016). Earlier research indicates that functional deficit in the visual system may be an initiating factor for cognitive impairment in MDD patients (Li et al., 2013). In addition, we observed decreased CBF in the insula, which plays a pivotal role in interoceptive awareness, emotional responses, and empathic processes (Menon & Uddin, 2010). This finding complements and extends prior literature on structural and functional impairments in this region in MDD (Liu et al., 2010; Stratmann et al., 2014). Collectively, our data suggest that there exists a cerebral perfusion redistribution across the reward circuitry, default-mode network, and visual system that might account for the clinical heterogeneity of MDD.

More importantly, leveraging transcription-neuroimaging spatial association analysis, we identified 1532 genes whose expression patterns were correlated with CBF changes in MDD. Functional enrichment analyses demonstrated that these genes were mainly enriched for ion channel (ion channel inhibitor activity and ion gated channel activity), synapse (syntaxin binding, signal release from synapse, and GABA-ergic synapse), neuron (neuron differentiation, neuronal cell body, and neuron projection), and neurotransmitter system (neurotransmitter receptor activity, GABA receptor activity, neurotransmitter transport, and neurotransmitter secretion). Ion channels are important for generating membrane potential, neuronal growth and differentiation, signal transduction, and neurotransmitter release (Kumar, Kumar, Jha, Jha, & Ambasta, 2016; Moody & Bosma, 2005; Smith & Walsh, 2020). Previous studies have suggested that ion channels, such as low-voltage-sensitive T-type calcium channel and potassium channel Kir4.1, hold promise as therapeutic targets for depression (Hashimoto, 2019). It is generally accepted that brain function relies on the ability of neurons to communicate with each other; inter-neuronal communication primarily takes place at synapses, where information from one neuron is rapidly conveyed to a second neuron (Pereda, 2014). Basic studies have documented that ketamine, a rapid antidepressant, can induce synaptogenesis and reverse synaptic deficits caused by chronic stress, highlighting the role of synaptic dysfunction in depression and its potential as a therapeutic target (Duman & Aghajanian, 2012). It is quite apparent that neuronal impairment and maldevelopment may be central to the neurology of depression (Krishnan & Nestler, 2008; Willner, Scheel-Krüger, & Belzung, 2013). Besides, neurons are a key component of the neurovascular unit, which serves as the structural basis of the coupling between CBF and neuronal activity. Central to brain health, neurovascular interactions have emerged as essential contributors to brain development and are vital for maintaining the homeostasis of the brain internal milieu (Iadecola, 2017). Accumulating data have indicated the occurrence of neurovascular coupling disruption in major psychiatric disorders including MDD (Segarra, Aburto, Hefendehl, & Acker-Palmer, 2019). Extensive research indicates that dysfunction of neurotransmitter systems (e.g. GABA, glutamate, and dopamine) has been implicated in the pathophysiology of MDD (Choudary et al., 2005; Grace, 2016; Klempan et al., 2009). Moreover, SAGE-217, a positive allosteric modulator of GABA type A receptors, has been proven to be effective for the treatment of MDD (Gunduz-Bruce et al., 2019). With respect to diseases, the genes related to CBF changes in MDD were found to be enriched for several mental disorders including depressive disorder, autistic disorder, bipolar disorder and schizophrenia, indicative of some common genetic mechanisms contributing to these illnesses.

Specific expression analyses showed that the genes associated with CBF changes in MDD were specifically expressed in the brain tissue, in immune cells and neurons, and during nearly all developmental stages. It is often assumed that immune cells (e.g. microglia) have the potential to regulate the development, structure, and function of neuronal networks in the brain (Garaschuk & Verkhratsky, 2019). In addition, immune cells have been evidenced to involve the establishment of the MDD model, emphasizing the neuroimmune mechanisms of depression (Hodes, Kana, Menard, Merad, & Russo, 2015). The specific expression in neurons echoes the aforementioned functional enrichment results. The temporal specific expression indicates that these genes exert an enduring effect on MDD-related CBF changes throughout nearly all cortical developmental stages. Regarding behavioral relevance, the genes related to CBF changes in MDD were associated with domains involving emotion and sensation. Deficits in these behavioral domains have been widely reported in MDD (Fam, Rush, Haaland, Barbier, & Luu, 2013; Rottenberg, 2017; Salmela et al., 2021). Of note, these genes could construct a PPI network supported by 60 putative hub genes with functional significance for understanding the pathology and treatment of MDD. For example, several G protein related genes (i.e. GNG2, GNB4, and GNG4) encode G protein coupled receptors (GPCRs), which could mediate the eukaryotic repertoire for cell communication and signal transduction. GPCRs are considered to be implicated in MDD (Mantas, Saarinen, Xu, & Svenningsson, 2022) and several novel antidepressants targeting GPCRs have been developed (Borroto-Escuela et al., 2021; Mantas et al., 2022).

Several limitations should be taken into account when interpreting our findings. First, most of the MDD patients in both the neuroimaging meta-analysis and the independent dataset were antidepressant-medicated and chronic, which may introduce confounds of antidepressant medication and illness duration. Future studies with drug-naïve first-episode patients with MDD are needed to eliminate these confounds and verify the preliminary findings. Second, the meta-analysis z map cannot reflect the nature and extent of whole-brain CBF differences between MDD patients and HC, because only peak coordinates and corresponding effect sizes of significant clusters reported in the previous literature were used. Third, the gene expression data were obtained from post-mortem brains, while the neuroimaging data were collected from living brains. Given the mounting

https://doi.org/10.1017/S0033291722003750 Published online by Cambridge University Press

evidence of conservative gene expression across individuals (Hawrylycz et al., 2015; Zeng et al., 2012), we set a DS threshold to focus on the genes with more conserved expression patterns, such that our transcription-neuroimaging spatial association analysis is feasible. However, some genes with great inter-subject variability in expression profiles would be missed. Fourth, considering limited gene expression data in the right hemisphere and substantial gene expression divergence between cortical and subcortical regions, we only included the tissue samples in the left cerebral cortex, which may have introduced potential biases. Finally, our neuroimaging meta-analysis results cannot survive multiple comparison correction. Instead, we reported our results by using a voxel-wise threshold of $p < 0.005$ combined with a cluster size threshold of 10 voxels to optimally balance Types I and II error rates following prior recommendation (Radua et al., 2012).

In conclusion, our data showed a cerebral perfusion redistribution in MDD, characterized by increased CBF in the reward circuitry and default-mode network and decreased CBF in the visual system. Further transcriptome-neuroimaging correlation analyses demonstrated that these CBF changes were spatially associated with expression of 1532 genes with diverse functional features. Our findings may not only offer unique insight into the genetic mechanisms of CBF changes in MDD, but also inform novel treatment approaches targeting the molecular substrates underlying brain phenotypes of this disorder.

Supplementary material. The supplementary material for this article can be found at https://doi.org/10.1017/S0033291722003750.

Acknowledgements. This work was supported by the National Natural Science Foundation of China (grant number: 82071905), the Natural Science Foundation of Anhui Province (grant number: 2208085MH257), the Outstanding Youth Support Project of Anhui Province Universities (grant number: gxyqZD2022026) and the Scientific Research Foundation of Anhui Medical University (grant number: 2022xkj143). We thank the Allen Institute for Brain Science founders and staff who supplied the brain expression data.

Conflict of interest. The authors declare no conflict of interests.

References

Albajes-Eizagirre, A., Solanes, A., Fullana, M. A., Ioannidis, J. P. A., Fusar-Poli, P., Torrent, C., … Radua, J. (2019a). Meta-analysis of voxel-based neuroimaging studies using seed-based d mapping with permutation of subject images (SDM-PSI). *Journal of Visualized Experiments, 153*, e59841. doi:10.3791/59841.

Albajes-Eizagirre, A., Solanes, A., Vieta, E., & Radua, J. (2019b). Voxel-based meta-analysis via permutation of subject images (PSI): Theory and implementation for SDM. *Neuroimage*, *186*, 174–184. doi:10.1016/j.neuroimage.2018.10.077.

Althubaity, N., Schubert, J., Martins, D., Yousaf, T., Nettis, M. A., Mondelli, V., … Veronese, M. (2022). Choroid plexus enlargement is associated with neuroinflammation and reduction of blood brain barrier permeability in depression. *Neuroimage Clinical*, *33*, 102926. doi:10.1016/j.nicl.2021.102926.

Anderson, K. M., Collins, M. A., Kong, R., Fang, K., Li, J., He, T., … Holmes, A. J. (2020). Convergent molecular, cellular, and cortical neuroimaging signatures of major depressive disorder. *Proceedings of the National Academy of Sciences of the United States of America*, *117*(40), 25138–25149. doi:10.1073/pnas.2008004117.

Arnatkeviciute, A., Fulcher, B. D., & Fornito, A. (2019). A practical guide to linking brain-wide gene expression and neuroimaging data. *Neuroimage*, *189*, 353–367. doi:10.1016/j.neuroimage.2019.01.011.

Bench, C. J., Friston, K. J., Brown, R. G., Scott, L. C., Frackowiak, R. S., & Dolan, R. J. (1992). The anatomy of melancholia--focal abnormalities of cerebral blood flow in major depression. *Psychological Medicine*, *22*(3), 607–615. doi:10.1017/s003329170003806x.

Bonte, F. J., Trivedi, M. H., Devous, M. D. Sr., Harris, T. S., Payne, J. K., Weinberg, W. A., & Haley, R. W. (2001). Occipital brain perfusion deficits in children with major depressive disorder. *Journal of Nuclear Medicine*, *42*(7), 1059–1061. Retrieved from https://pubmed.ncbi.nlm.nih.gov/11438629/.

Borroto-Escuela, D. O., Ambrogini, P., Narvaez, M., Di Liberto, V., Beggiato, S., Ferraro, L., … Fuxe, K. (2021). Serotonin heteroreceptor complexes and their integration of signals in neurons and astroglia-relevance for mental diseases. *Cells*, *10*(8), 1902. doi:10.3390/cells10081902.

Bromet, E., Andrade, L. H., Hwang, I., Sampson, N. A., Alonso, J., de Girolamo, G., … Kessler, R. C. (2011). Cross-national epidemiology of DSM-IV major depressive episode. *BMC Medicine*, *9*, 90. doi:10.1186/1741-7015-9-90.

Buckner, R. L., & DiNicola, L. M. (2019). The brain's default network: Updated anatomy, physiology and evolving insights. *Nature Reviews Neuroscience*, *20*(10), 593–608. doi:10.1038/s41583-019-0212-7.

Buxton, R. B. (2021). The thermodynamics of thinking: Connections between neural activity, energy metabolism and blood flow. *Philosophical Transactions of the Royal Society of London. Series B, Biological Sciences*, *376*(1815), 20190624. doi:10.1098/rstb.2019.0624.

Buxton, R. B., Frank, L. R., Wong, E. C., Siewert, B., Warach, S., & Edelman, R. R. (1998). A general kinetic model for quantitative perfusion imaging with arterial spin labeling. *Magnetic Resonance in Medicine*, *40*(3), 383–396. doi:10.1002/mrm.1910400308.

Cantisani, A., Stegmayer, K., Bracht, T., Federspiel, A., Wiest, R., Horn, H., … Walther, S. (2016). Distinct resting-state perfusion patterns underlie psychomotor retardation in unipolar vs. bipolar depression. *Acta Psychiatrica Scandinavica*, *134*(4), 329–338. doi:10.1111/acps.12625.

Chen, G., Bian, H., Jiang, D., Cui, M., Ji, S., Liu, M., … Zhuo, C. (2016). Pseudo-continuous arterial spin labeling imaging of cerebral blood perfusion asymmetry in drug-naive patients with first-episode major depression. *Biomedical Reports*, *5*(6), 675–680. doi:10.3892/br.2016.796.

Chen, J., Bardes, E. E., Aronow, B. J., & Jegga, A. G. (2009). ToppGene Suite for gene list enrichment analysis and candidate gene prioritization. *Nucleic Acids Research*, *37*(Web Server issue), W305–W311. doi:10.1093/nar/gkp427.

Chen, J., Zhang, C., Wang, R., Jiang, P., Cai, H., Zhao, W., … Yu, Y. (2022). Molecular basis underlying functional connectivity of fusiform gyrus subregions: A transcriptome-neuroimaging spatial correlation study. *Cortex*, *152*, 59–73. doi:10.1016/j.cortex.2022.03.016.

Chen, Z. Q., Du, M. Y., Zhao, Y. J., Huang, X. Q., Li, J., Lui, S., … Gong, Q. Y. (2015). Voxel-wise meta-analyses of brain blood flow and local synchrony abnormalities in medication-free patients with major depressive disorder. *Journal of Psychiatry & Neuroscience*, *40*(6), 401–411. doi:10.1503/jpn.140119.

Chithiramohan, T., Parekh, J. N., Kronenberg, G., Haunton, V. J., Minhas, J. S., Panerai, R. B., … Beishon, L. (2022). Investigating the association between depression and cerebral haemodynamics-A systematic review and meta-analysis. *Journal of Affective Disorders*, *299*, 144–158. doi:10.1016/j.jad.2021.11.037.

Choudary, P. V., Molnar, M., Evans, S. J., Tomita, H., Li, J. Z., Vawter, M. P., … Jones, E. G. (2005). Altered cortical glutamatergic and GABAergic signal transmission with glial involvement in depression. *Proceedings of the National Academy of Sciences of the United States of America*, *102*(43), 15653–15658. doi:10.1073/pnas.0507901102.

Clery-Melin, M. L., Jollant, F., & Gorwood, P. (2019). Reward systems and cognitions in major depressive disorder. *CNS Spectrums*, *24*(1), 64–77. doi:10.1017/S1092852918001335.

Consortium, C. (2015). Sparse whole-genome sequencing identifies two loci for major depressive disorder. *Nature*, *523*(7562), 588–591. doi:10.1038/nature14659.

Cooper, C. M., Chin Fatt, C. R., Liu, P., Grannemann, B. D., Carmody, T., Almeida, J. R. C., … Trivedi, M. H. (2020). Discovery and replication of cerebral blood flow differences in major depressive disorder. *Molecular Psychiatry*, *25*(7), 1500–1510. doi:10.1038/s41380-019-0464-7.

Corfield, E. C., Yang, Y., Martin, N. G., & Nyholt, D. R. (2017). A continuum of genetic liability for minor and major depression. *Translational Psychiatry*, *7*(5), e1131–e1131. doi:10.1038/tp.2017.99.

Dougherty, J. D., Schmidt, E. F., Nakajima, M., & Heintz, N. (2010). Analytical approaches to RNA profiling data for the identification of genes enriched in specific cells. *Nucleic Acids Research*, *38*(13), 4218–4230. doi:10.1093/nar/gkq130.

Duhameau, B., Ferre, J. C., Jannin, P., Gauvrit, J. Y., Verin, M., Millet, B., & Drapier, D. (2010). Chronic and treatment-resistant depression: A study using arterial spin labeling perfusion MRI at 3Tesla. *Psychiatry Research*, *182*(2), 111–116. doi:10.1016/j.pscychresns.2010.01.009.

Duman, R. S., & Aghajanian, G. K. (2012). Synaptic dysfunction in depression: Potential therapeutic targets. *Science (New York, N.Y.)*, *338*(6103), 68–72. doi:10.1126/science.1222939.

Fam, J., Rush, A. J., Haaland, B., Barbier, S., & Luu, C. (2013). Visual contrast sensitivity in major depressive disorder. *Journal of Psychosomatic Research*, *75*(1), 83–86. doi:10.1016/j.jpsychores.2013.03.008.

Fornito, A., Arnatkeviciute, A., & Fulcher, B. D. (2019). Bridging the gap between connectome and transcriptome. *Trends in Cognitive Sciences*, *23*(1), 34–50. doi:10.1016/j.tics.2018.10.005.

Gandal, M. J., Haney, J. R., Parikshak, N. N., Leppa, V., Ramaswami, G., Hartl, C., … Geschwind, D. H. (2018). Shared molecular neuropathology across major psychiatric disorders parallels polygenic overlap. *Science (New York, N.Y.)*, *359*(6376), 693–697. doi:10.1126/science.aad6469.

Garaschuk, O., & Verkhratsky, A. (2019). Physiology of microglia. *Methods in Molecular Biology (Clifton, N.J.)*, *2034*, 27–40. doi:10.1007/978-1-4939-9658-2_3.

Grace, A. A. (2016). Dysregulation of the dopamine system in the pathophysiology of schizophrenia and depression. *Nature Reviews Neuroscience*, *17*(8), 524–532. doi:10.1038/nrn.2016.57.

Greenberg, P. E., Fournier, A. A., Sisitsky, T., Simes, M., Berman, R., Koenigsberg, S. H., & Kessler, R. C. (2021). The economic burden of adults with major depressive disorder in the United States (2010 and 2018). *Pharmacoeconomics*, *39*(6), 653–665. doi:10.1007/s40273-021-01019-4.

Gunduz-Bruce, H., Silber, C., Kaul, I., Rothschild, A. J., Riesenberg, R., Sankoh, A. J., … Kanes, S. J. (2019). Trial of SAGE-217 in patients with major depressive disorder. *The New England Journal of Medicine*, *381*(10), 903–911. doi:10.1056/NEJMoa1815981.

Haller, S., Zaharchuk, G., Thomas, D. L., Lovblad, K. O., Barkhof, F., & Golay, X. (2016). Arterial spin labeling perfusion of the brain: Emerging clinical applications. *Radiology*, *281*(2), 337–356. doi:10.1148/radiol.2016150789.

Hamilton, J. P., Etkin, A., Furman, D. J., Lemus, M. G., Johnson, R. F., & Gotlib, I. H. (2012). Functional neuroimaging of major depressive disorder: A meta-analysis and new integration of base line activation and neural response data. *The American Journal of Psychiatry*, *169*(7), 693–703. doi:10.1176/appi.ajp.2012.11071105.

Hashimoto, K. (2019). Rapid-acting antidepressant ketamine, its metabolites and other candidates: A historical overview and future perspective. *Psychiatry and Clinical Neurosciences*, *73*(10), 613–627. doi:10.1111/pcn.12902.

Hawrylycz, M., Miller, J. A., Menon, V., Feng, D., Dolbeare, T., Guillozet-Bongaarts, A. L., … Lein, E. (2015). Canonical genetic signatures of the adult human brain. *Nature Neuroscience*, *18*(12), 1832–1844. doi:10.1038/nn.4171.

Hawrylycz, M. J., Lein, E. S., Guillozet-Bongaarts, A. L., Shen, E. H., Ng, L., Miller, J. A., … Jones, A. R. (2012). An anatomically comprehensive atlas of the adult human brain transcriptome. *Nature*, *489*(7416), 391–399. doi:10.1038/nature11405.

Hernandez-Garcia, L., Lahiri, A., & Schollenberger, J. (2019). Recent progress in ASL. *Neuroimage*, *187*, 3–16. doi:10.1016/j.neuroimage.2017.12.095.

Ho, T. C., Wu, J., Shin, D. D., Liu, T. T., Tapert, S. F., Yang, G., … Yang, T. T. (2013). Altered cerebral perfusion in executive, affective, and motor networks during adolescent depression. *Journal of the American Academy of Child & Adolescent Psychiatry*, *52*(10), 1076–1091.e2. doi:10.1016/j.jaac.2013.07.008.

Hodes, G. E., Kana, V., Menard, C., Merad, M., & Russo, S. J. (2015). Neuroimmune mechanisms of depression. *Nature Neuroscience*, *18*(10), 1386–1393. doi:10.1038/nn.4113.

Hoflich, A., Michenthaler, P., Kasper, S., & Lanzenberger, R. (2019). Circuit mechanisms of reward, anhedonia, and depression. *The International Journal of Neuropsychopharmacology*, *22*(2), 105–118. doi:10.1093/ijnp/pyy081.

Howard, D. M., Adams, M. J., Clarke, T. K., Hafferty, J. D., Gibson, J., Shirali, M., … McIntosh, A. M. (2019). Genome-wide meta-analysis of depression identifies 102 independent variants and highlights the importance of the prefrontal brain regions. *Nature Neuroscience*, *22*(3), 343–352. doi:10.1038/s41593-018-0326-7.

Howard, D. M., Adams, M. J., Shirali, M., Clarke, T. K., Marioni, R. E., Davies, G., … McIntosh, A. M. (2018). Genome-wide association study of depression phenotypes in UK Biobank identifies variants in excitatory synaptic pathways. *Nature Communications*, *9*(1), 1470. doi:10.1038/s41467-018-03819-3.

Hyde, C. L., Nagle, M. W., Tian, C., Chen, X., Paciga, S. A., Wendland, J. R., … Winslow, A. R. (2016). Identification of 15 genetic loci associated with risk of major depression in individuals of European descent. *Nature Genetics*, *48*(9), 1031–1036. doi:10.1038/ng.3623.

Iadecola, C. (2017). The neurovascular unit coming of age: A journey through neurovascular coupling in health and disease. *Neuron*, *96*(1), 17–42. doi:10.1016/j.neuron.2017.07.030.

Jarnum, H., Eskildsen, S. F., Steffensen, E. G., Lundbye-Christensen, S., Simonsen, C. W., Thomsen, I. S., … Larsson, E. M. (2011). Longitudinal MRI study of cortical thickness, perfusion, and metabolite levels in major depressive disorder. *Acta Psychiatrica Scandinavica*, *124*(6), 435–446. doi:10.1111/j.1600-0447.2011.01766.x.

Ji, Y., Zhang, X., Wang, Z., Qin, W., Liu, H., Xue, K., … Yu, C. (2021). Genes associated with gray matter volume alterations in schizophrenia. *Neuroimage*, *225*, 117526. doi:10.1016/j.neuroimage.2020.117526.

Kaichi, Y., Okada, G., Takamura, M., Toki, S., Akiyama, Y., Higaki, T., … Awai, K. (2016). Changes in the regional cerebral blood flow detected by arterial spin labeling after 6-week escitalopram treatment for major depressive disorder. *Journal of Affective Disorders*, *194*, 135–143. doi:10.1016/j.jad.2015.12.062.

Kessler, R. C., & Bromet, E. J. (2013). The epidemiology of depression across cultures. *Annual Review of Public Health*, *34*, 119–138. doi:10.1146/annurev-publhealth-031912-114409.

Klempan, T. A., Sequeira, A., Canetti, L., Lalovic, A., Ernst, C., ffrench-Mullen, J., & Turecki, G. (2009). Altered expression of genes involved in ATP biosynthesis and GABAergic neurotransmission in the ventral prefrontal cortex of suicides with and without major depression. *Molecular Psychiatry*, *14*(2), 175–189. doi:10.1038/sj.mp.4002110.

Krausz, Y., Freedman, N., Lester, H., Barkai, G., Levin, T., Bocher, M., … Bonne, O. (2007). Brain SPECT study of common ground between hypothyroidism and depression. *The International Journal of Neuropsychopharmacology*, *10*(1), 99–106. doi:10.1017/S1461145706006481.

Krishnan, V., & Nestler, E. J. (2008). The molecular neurobiology of depression. *Nature*, *455*(7215), 894–902. doi:10.1038/nature07455.

Kumar, P., Kumar, D., Jha, S. K., Jha, N. K., & Ambasta, R. K. (2016). Ion channels in neurological disorders. *Advances in Protein Chemistry and Structural Biology*, *103*, 97–136. doi:10.1016/bs.apcsb.2015.10.006.

Lancaster, J. L., Tordesillas-Gutierrez, D., Martinez, M., Salinas, F., Evans, A., Zilles, K., … Fox, P. T. (2007). Bias between MNI and Talairach coordinates analyzed using the ICBM-152 brain template. *Human Brain Mapping*, *28*(11), 1194–1205. doi:10.1002/hbm.20345.

Lecrux, C., Bourourou, M., & Hamel, E. (2019). How reliable is cerebral blood flow to map changes in neuronal activity? *Autonomic Neuroscience*, *217*, 71–79. doi:10.1016/j.autneu.2019.01.005.

Li, J., Seidlitz, J., Suckling, J., Fan, F., Ji, G. J., Meng, Y., … Liao, W. (2021). Cortical structural differences in major depressive disorder correlate with cell type-specific transcriptional signatures. *Nature Communications*, *12*(1), 1647. doi:10.1038/s41467-021-21943-5.

Li, J., Xu, C., Cao, X., Gao, Q., Wang, Y., Wang, Y., … Zhang, K. (2013). Abnormal activation of the occipital lobes during emotion picture processing in major depressive disorder patients. *Neural Regeneration Research*, *8*(18), 1693–1701. doi:10.3969/j.issn.1673-5374.2013.18.007.

Li, J., Yang, Y., Zhu, Y., Zhou, L., Han, Y., Yin, T., … Chen, J. (2018). Towards characterizing the regional cerebral perfusion in evaluating the severity of major depression disorder with SPECT/CT. *BMC Psychiatry*, *18*(1), 70. doi:10.1186/s12888-018-1654-6.

Li, W., Chen, Z., Wu, M., Zhu, H., Gu, L., Zhao, Y., … Gong, Q. (2017). Characterization of brain blood flow and the amplitude of low-frequency

https://doi.org/10.1017/S0033291722003750 Published online by Cambridge University Press

fluctuations in major depressive disorder: A multimodal meta-analysis. *Journal of Affective Disorders*, *210*, 303–311. doi:10.1016/j.jad.2016.12.032.
Lieberman, M. D., & Cunningham, W. A. (2009). Type I and Type II error concerns in fMRI research: Re-balancing the scale. *Social Cognitive and Affective Neuroscience*, *4*(4), 423–428. doi:10.1093/scan/nsp052.
Liu, F., Tian, H., Li, J., Li, S., & Zhuo, C. (2019). Altered voxel-wise gray matter structural brain networks in schizophrenia: Association with brain genetic expression pattern. *Brain Imaging and Behavior*, *13*(2), 493–502. doi:10.1007/s11682-018-9880-6.
Liu, S., Zhang, C., Meng, C., Wang, R., Jiang, P., Cai, H., … Zhu, J. (2022). Frequency-dependent genetic modulation of neuronal oscillations: A combined transcriptome and resting-state functional MRI study. *Cerebral cortex*, *32*(22), 5132–5144. doi:10.1093/cercor/bhac003.
Liu, Z., Xu, C., Xu, Y., Wang, Y., Zhao, B., Lv, Y., … Du, C. (2010). Decreased regional homogeneity in insula and cerebellum: A resting-state fMRI study in patients with major depression and subjects at high risk for major depression. *Psychiatry Research*, *182*(3), 211–215. doi:10.1016/j.pscychresns.2010.03.004.
Lui, S., Parkes, L. M., Huang, X., Zou, K., Chan, R. C., Yang, H., … Gong, Q. Y. (2009). Depressive disorders: Focally altered cerebral perfusion measured with arterial spin-labeling MR imaging. *Radiology*, *251*(2), 476–484. doi:10.1148/radiol.2512081548.
Malhi, G. S., & Mann, J. J. (2018). Depression. *Lancet (London, England)*, *392* (10161), 2299–2312. doi:10.1016/s0140-6736(18)31948-2.
Mantas, I., Saarinen, M., Xu, Z. D., & Svenningsson, P. (2022). Update on GPCR-based targets for the development of novel antidepressants. *Molecular Psychiatry*, *27*(1), 534–558. doi:10.1038/s41380-021-01040-1.
Menon, V., & Uddin, L. Q. (2010). Saliency, switching, attention and control: A network model of insula function. *Brain Structure and Function*, *214*(5–6), 655–667. doi:10.1007/s00429-010-0262-0.
Moher, D., Liberati, A., Tetzlaff, J., Altman, D. G., & Group, P. (2009). Preferred reporting items for systematic reviews and meta-analyses: The PRISMA statement. *PLoS Medicine*, *6*(7), e1000097. doi:10.1371/journal.pmed.1000097.
Monkul, E. S., Silva, L. A., Narayana, S., Peluso, M. A., Zamarripa, F., Nery, F. G., … Soares, J. C. (2012). Abnormal resting state corticolimbic blood flow in depressed unmedicated patients with major depression: A (15)O-H(2)O PET study. *Human Brain Mapping*, *33*(2), 272–279. doi:10.1002/hbm.21212.
Moody, W. J., & Bosma, M. M. (2005). Ion channel development, spontaneous activity, and activity-dependent development in nerve and muscle cells. *Physiological Reviews*, *85*(3), 883–941. doi:10.1152/physrev.00017.2004.
Muller, V. I., Cieslik, E. C., Laird, A. R., Fox, P. T., Radua, J., Mataix-Cols, D., … Eickhoff, S. B. (2018). Ten simple rules for neuroimaging meta-analysis. *Neuroscience and Biobehavioral Reviews*, *84*, 151–161. doi:10.1016/j.neubiorev.2017.11.012.
Nagafusa, Y., Okamoto, N., Sakamoto, K., Yamashita, F., Kawaguchi, A., Higuchi, T., & Matsuda, H. (2012). Assessment of cerebral blood flow findings using 99mTc-ECD single-photon emission computed tomography in patients diagnosed with major depressive disorder. *Journal of Affective Disorders*, *140*(3), 296–299. doi:10.1016/j.jad.2012.03.026.
Nestler, E. J., & Carlezon, W. A. Jr. (2006). The mesolimbic dopamine reward circuit in depression. *Biological Psychiatry*, *59*(12), 1151–1159. doi:10.1016/j.biopsych.2005.09.018.
Ota, M., Noda, T., Sato, N., Hattori, K., Teraishi, T., Hori, H., … Kunugi, H. (2014). Characteristic distributions of regional cerebral blood flow changes in major depressive disorder patients: A pseudo-continuous arterial spin labeling (pCASL) study. *Journal of Affective Disorders*, *165*, 59–63. doi:10.1016/j.jad.2014.04.032.
Pereda, A. E. (2014). Electrical synapses and their functional interactions with chemical synapses. *Nature Reviews Neuroscience*, *15*(4), 250–263. doi:10.1038/nrn3708.
Périco, C. A.-M., Skaf, C. R., Yamada, A., Duran, F., Buchpiguel, C. A., Castro, C. C., … Busatto, G. F. (2005). Relationship between regional cerebral blood flow and separate symptom clusters of major depression: A single photon emission computed tomography study using statistical parametric mapping. *Neuroscience Letters*, *384*(3), 265–270. doi:10.1016/j.neulet.2005.04.088.
Pizzagalli, D. A., Holmes, A. J., Dillon, D. G., Goetz, E. L., Birk, J. L., Bogdan, R., … Fava, M. (2009). Reduced caudate and nucleus accumbens response to rewards in unmedicated individuals with major depressive disorder. *The American Journal of Psychiatry*, *166*(6), 702–710. doi:10.1176/appi.ajp.2008.08081201.
Prasad, S., & Galetta, S. L. (2011). Anatomy and physiology of the afferent visual system. *Handbook of Clinical Neurology*, *102*, 3–19. doi:10.1016/B978-0-444-52903-9.00007-8.
Radua, J., Mataix-Cols, D., Phillips, M. L., El-Hage, W., Kronhaus, D. M., Cardoner, N., & Surguladze, S. (2012). A new meta-analytic method for neuroimaging studies that combines reported peak coordinates and statistical parametric maps. *European Psychiatry*, *27*(8), 605–611. doi:10.1016/j.eurpsy.2011.04.001.
Raichle, M. E. (2015). The brain's default mode network. *Annual Review of Neuroscience*, *38*, 433–447. doi:10.1146/annurev-neuro-071013-014030.
Rappaport, N., Twik, M., Plaschkes, I., Nudel, R., Iny Stein, T., Levitt, J., … Lancet, D. (2017). MalaCards: An amalgamated human disease compendium with diverse clinical and genetic annotation and structured search. *Nucleic Acids Research*, *45*(D1), D877–D887. doi:10.1093/nar/gkw1012.
Ripke, S., Wray, N. R., Lewis, C. M., Hamilton, S. P., Weissman, M. M. Breen, G., … Sullivan, P. F. (2013). A mega-analysis of genome-wide association studies for major depressive disorder. *Molecular Psychiatry*, *18*(4), 497–511. doi:10.1038/mp.2012.21.
Roelfsema, P. R., & de Lange, F. P. (2016). Early visual cortex as a multiscale cognitive blackboard. *Annual Review of Vision Science*, *2*, 131–151. doi:10.1146/annurev-vision-111815-114443.
Romero-Garcia, R., Warrier, V., Bullmore, E. T., Baron-Cohen, S., & Bethlehem, R. A. I. (2019). Synaptic and transcriptionally downregulated genes are associated with cortical thickness differences in autism. *Molecular Psychiatry*, *24*(7), 1053–1064. doi:10.1038/s41380-018-0023-7.
Rottenberg, J. (2017). Emotions in depression: What do we really know? *Annual Review of Clinical Psychology*, *13*, 241–263. doi:10.1146/annurev-clinpsy-032816-045252.
Russo, S. J., & Nestler, E. J. (2013). The brain reward circuitry in mood disorders. *Nature Reviews Neuroscience*, *14*(9), 609–625. doi:10.1038/nrn3381.
Sahib, A. K., Loureiro, J. R. A., Vasavada, M. M., Kubicki, A., Joshi, S. H., Wang, K., … Narr, K. L. (2020). Single and repeated ketamine treatment induces perfusion changes in sensory and limbic networks in major depressive disorder. *European Neuropsychopharmacology*, *33*, 89–100. doi:10.1016/j.euroneuro.2020.01.017.
Salmela, V., Socada, L., Soderholm, J., Heikkila, R., Lahti, J., Ekelund, J., & Isometsa, E. (2021). Reduced visual contrast suppression during major depressive episodes. *Journal of Psychiatry and Neuroscience*, *46*(2), E222–E231. doi:10.1503/jpn.200091.
Savitz, J., Nugent, A. C., Cannon, D. M., Carlson, P. J., Davis, R., Neumeister, A., … Drevets, W. C. (2012). Effects of arterial cannulation stress on regional cerebral blood flow in major depressive disorder. *Scientific Reports*, *2*, 308. doi:10.1038/srep00308.
Segarra, M., Aburto, M. R., Hefendehl, J., & Acker-Palmer, A. (2019). Neurovascular interactions in the nervous system. *Annual Review of Cell and Developmental Biology*, *35*, 615–635. doi:10.1146/annurev-cellbio-100818-125142.
Smith, R. S., & Walsh, C. A. (2020). Ion channel functions in early brain development. *Trends in Neurosciences*, *43*(2), 103–114. doi:10.1016/j.tins.2019.12.004.
Stratmann, M., Konrad, C., Kugel, H., Krug, A., Schoning, S., Ohrmann, P., … Dannlowski, U. (2014). Insular and hippocampal gray matter volume reductions in patients with major depressive disorder. *PLoS One*, *9*(7), e102692. doi:10.1371/journal.pone.0102692.
Sullivan, P. F., Neale, M. C., & Kendler, K. S. (2000). Genetic epidemiology of major depression: Review and meta-analysis. *The American Journal of Psychiatry*, *157*(10), 1552–1562. doi:10.1176/appi.ajp.157.10.1552.
Tao, H., Guo, S., Ge, T., Kendrick, K. M., Xue, Z., Liu, Z., … Feng, J. (2013). Depression uncouples brain hate circuit. *Molecular Psychiatry*, *18*(1), 101–111. doi:10.1038/mp.2011.127.
Vardi, N., Freedman, N., Lester, H., Gomori, J. M., Chisin, R., Lerer, B., & Bonne, O. (2011). Hyperintensities on T2-weighted images in the basal ganglia of patients with major depression: Cerebral perfusion and clinical implications. *Psychiatry Research*, *192*(2), 125–130. doi:10.1016/j.pscychresns.2010.11.010.

https://doi.org/10.1017/S0033291722003750 Published online by Cambridge University Press

Vasic, N., Wolf, N. D., Gron, G., Sosic-Vasic, Z., Connemann, B. J., Sambataro, F., … Wolf, R. C. (2015). Baseline brain perfusion and brain structure in patients with major depression: A multimodal magnetic resonance imaging study. *Journal of Psychiatry & Neuroscience*, *40*(6), 412–421. doi:10.1503/jpn.140246.

Wang, Y. M., & Yang, Z. Y. (2022). Aberrant pattern of cerebral blood flow in patients with major depressive disorder: A meta-analysis of arterial spin labelling studies. *Psychiatry Research Neuroimaging*, *321*, 111458. doi:10.1016/j.pscychresns.2022.111458.

Whiteford, H. A., Degenhardt, L., Rehm, J., Baxter, A. J., Ferrari, A. J., Erskine, H. E., … Vos, T. (2013). Global burden of disease attributable to mental and substance use disorders: Findings from the Global Burden of Disease Study 2010. *Lancet (London, England)*, *382*(9904), 1575–1586. doi:10.1016/s0140-6736(13)61611-6.

Whitmer, A. J., & Gotlib, I. H. (2013). An attentional scope model of rumination. *Psychological Bulletin*, *139*(5), 1036–1061. doi:10.1037/a0030923.

Willner, P., Scheel-Krüger, J., & Belzung, C. (2013). The neurobiology of depression and antidepressant action. *Neuroscience and Biobehavioral Reviews*, *37*(10 Pt 1), 2331–2371. doi:10.1016/j.neubiorev.2012.12.007.

Wintermark, M., Sesay, M., Barbier, E., Borbély, K., Dillon, W. P., Eastwood, J. D., … Yonas, H. (2005). Comparative overview of brain perfusion imaging techniques. *Journal of Neuroradiology*, *32*(5), 294–314. doi:10.1016/s0150-9861(05)83159-1.

World Health Organization. (2008). *The global burden of disease: 2004 update*. Geneva: World Health Organization. Retrieved from https://www.who.int/evidence/bod.

Wray, N. R., Ripke, S., Mattheisen, M., Trzaskowski, M., Byrne, E. M., Abdellaoui, A., … Sullivan, P. F. (2018). Genome-wide association analyses identify 44 risk variants and refine the genetic architecture of major depression. *Nature Genetics*, *50*(5), 668–681. doi:10.1038/s41588-018-0090-3.

Xie, Y., Zhang, X., Liu, F., Qin, W., Fu, J., Xue, K., & Yu, C. (2020). Brain mRNA expression associated with cortical volume alterations in autism spectrum disorder. *Cell Reports*, *32*(11), 108137. doi:10.1016/j.celrep.2020.108137.

Xu, G., Rowley, H. A., Wu, G., Alsop, D. C., Shankaranarayanan, A., Dowling, M., … Johnson, S. C. (2010). Reliability and precision of pseudo-continuous arterial spin labeling perfusion MRI on 3.0T and comparison with 15O-water PET in elderly subjects at risk for Alzheimer's disease. *NMR in Biomedicine*, *23*(3), 286–293. doi:10.1002/nbm.1462.

Xu, X., Wells, A. B., O'Brien, D. R., Nehorai, A., & Dougherty, J. D. (2014). Cell type-specific expression analysis to identify putative cellular mechanisms for neurogenetic disorders. *The Journal of Neuroscience*, *34*(4), 1420–1431. doi:10.1523/JNEUROSCI.4488-13.2014.

Xue, K., Liang, S., Yang, B., Zhu, D., Xie, Y., Qin, W., … Yu, C. (2020). Local dynamic spontaneous brain activity changes in first-episode, treatment-naive patients with major depressive disorder and their associated gene expression profiles. *Psychological Medicine*, *52*(11), 2052–2061. doi:10.1017/S0033291720003876.

Yarkoni, T., Poldrack, R. A., Nichols, T. E., Van Essen, D. C., & Wager, T. D. (2011). Large-scale automated synthesis of human functional neuroimaging data. *Nature Methods*, *8*(8), 665–670. doi:10.1038/nmeth.1635.

Yeshurun, Y., Nguyen, M., & Hasson, U. (2021). The default mode network: Where the idiosyncratic self meets the shared social world. *Nature Reviews Neuroscience*, *22*(3), 181–192. doi:10.1038/s41583-020-00420-w.

Zeng, H., Shen, E. H., Hohmann, J. G., Oh, S. W., Bernard, A., Royall, J. J., … Jones, A. R. (2012). Large-scale cellular-resolution gene profiling in human neocortex reveals species-specific molecular signatures. *Cell*, *149*(2), 483–496. doi:10.1016/j.cell.2012.02.052.

Zhang, C., Cai, H., Xu, X., Li, Q., Li, X., Zhao, W., … Yu, Y. (2021). Genetic architecture underlying differential resting-state functional connectivity of subregions within the human visual cortex. *Cerebral Cortex*, *32*(10), 2063–2078. doi:10.1093/cercor/bhab335.

Zhou, H. X., Chen, X., Shen, Y. Q., Li, L., Chen, N. X., Zhu, Z. C., … Yan, C. G. (2020). Rumination and the default mode network: Meta-analysis of brain imaging studies and implications for depression. *Neuroimage*, *206*, 116287. doi:10.1016/j.neuroimage.2019.116287.

Zhu, J., Zhuo, C., Qin, W., Xu, Y., Xu, L., Liu, X., & Yu, C. (2015). Altered resting-state cerebral blood flow and its connectivity in schizophrenia. *Journal of Psychiatric Research*, *63*, 28–35. doi:10.1016/j.jpsychires.2015.03.002.

Zhu, J., Zhuo, C., Xu, L., Liu, F., Qin, W., & Yu, C. (2017). Altered coupling between resting-state cerebral blood flow and functional connectivity in schizophrenia. *Schizophrenia Bulletin*, *43*(6), 1363–1374. doi:10.1093/schbul/sbx051.

Zhuo, C., Zhu, J., Qin, W., Qu, H., Ma, X., & Yu, C. (2017). Cerebral blood flow alterations specific to auditory verbal hallucinations in schizophrenia. *The British Journal of Psychiatry*, *210*(3), 209–215. doi:10.1192/bjp.bp.115.174961.

https://doi.org/10.1017/S0033291722003750 Published online by Cambridge University Press